ELSEVIER

Surface Science 383 (1997) 57–68

surface science

# The surface chemistry of ethylene adsorbed on Mo(100), oxygen-covered Mo(100) and $MoO_2$

G. Wu, B. Bartlett, W.T. Tysoe *

*Department of Chemistry and Laboratory for Surface Studies, University of Wisconsin-Milwaukee, Milwaukee, WI 53211, USA*

Received 25 November 1996; accepted for publication 22 January 1997

**Abstract**

Ethylene adsorbed on Mo(100) and oxygen-covered Mo(100) can thermally decompose to yield hydrogen and adsorbed carbon, desorb molecularly, self-hydrogenate to produce ethane or dissociate to form adsorbed $C_1$ species which can hydrogenate to form methane. Complete thermal decomposition of the ethylene is proposed to take place on the four-fold sites on Mo(100) since the hydrogen yield decreases linearly with oxygen coverage. The ethylene desorption activation energy increases with increasing oxygen coverage suggesting that ethylene bonds to Mo(100) predominantly by donation of $\pi$ electrons to the molybdenum surface. The ethylene hydrogenation activation increases as a function of oxygen coverage in accord with this effect. The yield of methane also varies with oxygen coverage so that no methane desorption is detected for clean Mo(100) but the yield increases with oxygen coverage reaching a maximum at a coverage of $\sim$0.6 ML and decreasing at higher coverages. Photoelectron spectroscopy results suggest that adsorbed oxygen increases the dissociative probability of ethylene. In addition, experiments in which carbenes are grafted onto the surface by decomposing methylene iodide show that carbenes are stabilized by the addition of oxygen to the surface. These effects both explain the increase in methane yield as a function of increasing oxygen coverage. The decrease at higher coverage is likely due, at least in part, to the lack of hydrogen. The ethane yield also decreases at higher coverages due to a similar effect.


*Keywords:* Alkenes; Catalysis; Low index single crystal surfaces; Models of surface chemical reactions; Molybdenum; Photoelectron spectroscopy; Single crystal surfaces; Thermal desorption spectroscopy; Visible and ultraviolet photoelectron spectroscopy

## 1. Introduction

Molybdenum provides the basis for a number of important catalytic materials, particularly when chemically modified, so that $MoS_2$ is an effective hydrodesulfurization catalyst [1,2] and oxidized molybdenum is active for the metathesis of olefins [3–6]. The metathesis reaction is catalyzed both in homogeneous and heterogeneous phase. In homogeneous phase, the reaction has been proposed to proceed via the initial formation of a carbene. This has been suggested to further react with an alkene forming a metallacycle which decomposes via the reverse of this route to form metathesis products [7–15]. In this case, the carbene acts as a catalytic "active site". The heterogeneous analog of this reaction was discovered a number of years ago by Banks and Bailey where the catalyst consisted of an alumina-supported molybdenum oxide [16]. It is generally accepted that the heterogeneous reaction proceeds via a similar "carbene–metallacycle" mechanism. Reaction studies carried out in an isolatable, high-

* Corresponding author. Fax: (+1) 414 229-5530; e-mail: wtt@alpha2.csd.uwm.edu

0039-6028/97/$17.00 
*PII* S0039-6028(97)00113-1

pressure reactor incorporated into an ultrahigh vacuum (UHV) chamber using thin molybdenum oxide films deposited onto a molybdenum substrate showed that either $MoO_2$ or $MoO_3$ provided the most active catalyst depending on reaction conditions [15,17,18]. Interestingly, two apparently quite different reaction regimes were encountered depending on temperature. Above $\sim$650 K, the activation energy was $\sim$65 kcal mol$^{-1}$, a value close to that found for catalysis on the clean metal. Below $\sim$650 K, in a temperature regime that metathesis is generally carried out using the supported catalyst [16], the reaction proceeded with a much lower activation energy ($\sim$6 kcal mol$^{-1}$) and high selectivity where the absolute reaction rates for the model catalyst were very close to values for a supported catalyst [17].

It was further found that reaction of ethylene catalyzed by metallic molybdenum yielded high-molecular-weight products (up to $C_8$) where the distribution was well described by a Schulz–Flory function indicating that products are formed by polymerization of a $C_1$ surface species [19]. It has previously been shown using ultraviolet photoelectron spectroscopy that ethylene rapidly dissociates into adsorbed $C_1$ species on metallic molybdenum [20], suggesting that their polymerization leads to the formation of higher molecular weight hydrocarbons on metallic molybdenum.

It is also found that oxygen overlayers affect the olefin metathesis activity for reaction above $\sim$650 K in a similar manner as the model oxides [5]. In this case it is found that the activity of oxygen-covered molybdenum increases up to an oxygen coverage of $\sim$0.6 ML and then decreases at higher oxygen coverages. Oxygen overlayers have the advantage, from the point of view of fundamental studies, of exhibiting well-ordered LEED patterns, and so are characterized by better defined structures than the oxides. The following paper examines the chemistry of ethylene, the simplest possible metathesis reactant, on oxygen-modified model molybdenum catalysts in ultrahigh vacuum using primarily temperature-programmed desorption and ultraviolet photoelectron spectroscopies to probe the surface chemistry of the adsorbed alkene. The 2p-derived molecular orbitals of adsorbed hydrocarbons are effectively obscured by photoemission features from the oxygen 2p levels of the adsorbed overlayer, particularly for high oxygen coverages. The C 2s-derived levels lie at a considerably higher binding energy than these levels but are somewhat lower in energy than the oxygen 2s levels so can be detected on an oxygen-covered surface. It has also been demonstrated that the positions of these levels can be quantitatively described using simple Hückel theory in the gas-phase [21]. Final-state effects mean that these levels cannot be used for a similar quantitative calculation of the ionization energies of 2s-derived molecular orbitals. They can, however, be used to follow chemical changes on the surface and are particularly useful for following gross molecular reorganizations, for example, carbon–carbon bond scission [21].

## 2. Experimental

Two pieces of equipment were used for these experiments which have been described in detail elsewhere [22,23]. Briefly, the first consists of an ion- and sublimation-pumped, bakeable, ultrahigh vacuum chamber operating at a base pressure of $<1\times10^{-10}$ Torr following bakeout. The Mo(100) sample is mounted to the end of a rotatable manipulator by means of 0.5 mm diameter tantalum heating wire that is spot-welded to 2 mm diameter tantalum rods. In addition, the manipulator has been retrofitted with electron-beam heating. In this case, a tungsten filament is placed just behind the sample and the sample is raised to a large positive potential ($\sim$500 V) with the filament heated. This allows the sample to be repeatedly heated to 2000 K without any adverse effects on the heating wires. The sample could also be cooled to $\sim$80 K via thermal contact to a liquid-nitrogen filled reservoir. Resistive heating was used to collect temperature-programmed desorption (TPD) data. These were collected using a computer-multiplexed quadrupole mass spectrometer that could record up to five masses sequentially using a heating rate of 10 K s$^{-1}$. The analyzer head of the quadrupole was enclosed in an evacuated shroud with a 1 cm diameter hole in the front to minimize signals not arising from the sample entering the mass spectrometer ionizer.

The chamber was also equipped with a four-grid retarding field analyzer (RFA) which was used to obtain LEED images of the sample and to collect Auger data. The sample was cleaned by heating in $\sim 2.5 \times 10^{-7}$ Torr of oxygen at 1200 K for five minutes to remove carbon and then rapidly heated in vacuo to 2100 K to remove oxygen. This resulted in the diffusion of further carbon to the surface and this procedure was repeated until no impurities, particularly carbon, were noted on the surface after heating to 2100 K.

Ultraviolet photoelectron spectra were obtained at the Wisconsin Synchrotron Radiation Center using the Aladdin storage ring. The stainless steel, ultra-high vacuum chamber used for these experiments operated at a base pressure of $\sim 1 \times 10^{-10}$ Torr following bakeout and was attached to the end of a Mark V Grasshopper monochromator. The chamber was equipped with a quadrupole mass analyzer for residual gas analysis and to test gas purities. It was also equipped with a double-pass cylindrical mirror analyzer which was used to collect both Auger and photoelectron spectra. Auger spectra were excited using a 3 keV electron beam and collected by pulse counting the scattered electrons and the $dn(E)/dE$ Auger spectrum obtained by numerically differentiating the $n(E)$ signal. The analyzer was operated at a pass energy of 25 eV to collect photoelectron spectra and this yielded an overall spectral resolution of 0.15 eV. They were excited using 60 eV radiation which has been shown previously to yield the optimum C 2s to background intensity ratio on Mo(100) [21].

The ethylene (Aldrich, 99.9% purity) was transferred to a glass bottle and further purified by repeated bulb-to-bulb distillations and stored in glass until use. The oxygen (AGA Gas, Inc. 99%) was transferred from the cylinder to a glass bulb and also redistilled.

Oxygen overlayers were prepared by saturating the Mo(100) surface (20 L $O_2$ exposure at 1050 K; 1 L $= 1 \times 10^{-6}$ Torr s) and annealing to various temperatures to remove oxygen to obtain the requisite coverage. The adsorption of oxygen on Mo(100) has been studied very extensively [24–27] and the oxygen coverages were reproduced from their characteristic LEED patterns and confirmed from their relative O/Mo Auger ratios (by monitoring the O KLL and Mo LMM Auger transitions). $MoO_2$ films were grown using a literature protocol [28] which provides a surface that is active for olefin metathesis where metallic molybdenum was oxidized using $3 \times 10^{-5}$ Torr of oxygen for 120 s with the sample heated to 1050 K.

## 3. Results

Various oxygen overlayers of different coverages were obtained by annealing an oxygen-saturated p(1 × 1) surface to various temperatures. These consisted of a (2 × 1) surface obtained by annealing at 1600 K to yield an oxygen coverage $\theta_O = 1.1$ ML, a $(\sqrt{5} \times \sqrt{5})$ pattern producing an oxygen coverage $\theta_O = 0.83$ ML and a (4 × 4) surface giving $\theta_O = 0.2$ ML. These LEED patterns reproduced those found by other workers [24–27]. $MoO_2$ is synthesized as described above. Finally, the relative oxygen coverages were checked by measuring the O/Mo Auger ratio as a function of annealing temperature. Note that $MoO_2$ provides a model catalyst that mimics the metathesis activity of high loadings of molybdenum oxide supported on alumina and the metathesis activity of metallic molybdenum modified by oxygen overlayers has been shown to increase as a function of oxygen coverage from $\theta_O = 0$ ML (clean surface) to $\theta_O = 0.6$ ML and decrease thereafter [5].

Photoelectron spectra of ethylene adsorbed on the various model catalysts were collected after saturating with ethylene (10 L exposure) and annealing to various temperatures for 5 s. The sample was then allowed to cool to 80 K after which the spectrum was recorded to prevent further chemical changes from occurring. Shown in Fig. 1 is the spectrum of ethylene adsorbed on $MoO_2$ displaying the C and O 2s region up to 27 eV binding energy (BE). The annealing temperature is displayed adjacent to each spectrum and a spectrum of $MoO_2$ prior to ethylene adsorption is shown for comparison. The intense peak at $22.5 \pm 0.2$ eV is assigned to emission from oxygen 2s orbitals and the broad structure between 5 and 10 eV binding energy is due to emission from O 2p orbitals. Features below ~3 eV BE are due to

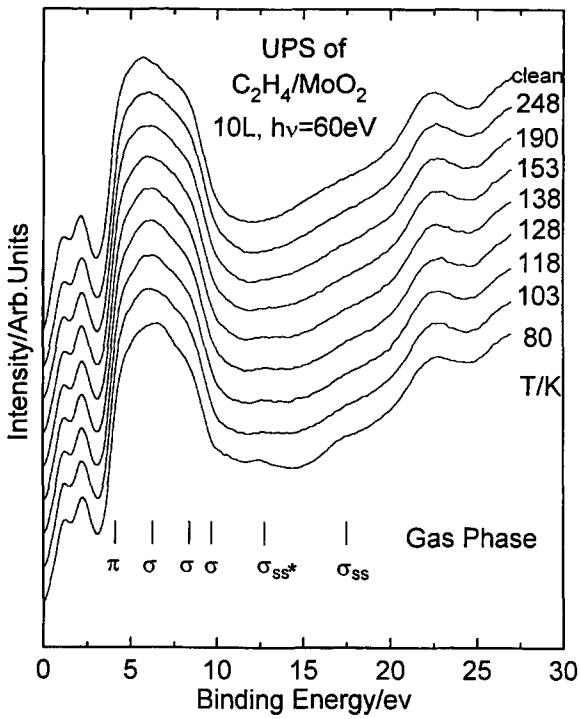


Fig. 1. Ultraviolet photoelectron spectra displaying the carbon and oxygen 2s region obtained following ethylene adsorption (10 L) on an $MoO_2$ surface as a function of sample annealing temperature. The annealing temperature is displayed adjacent to the corresponding spectrum. These spectra were excited using 60-eV photons.

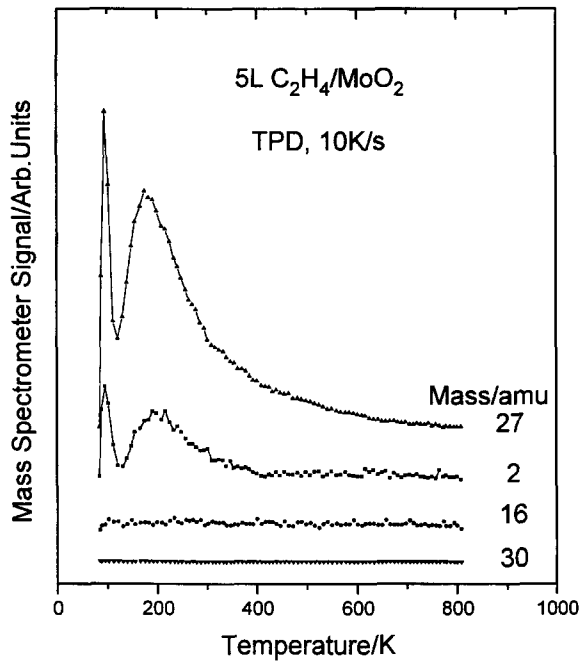


Fig. 2. Temperature-programmed desorption spectra collected at several masses following exposure of $MoO_2$ to 5 L of ethylene. The masses monitored are displayed adjacent to the corresponding spectrum.

emission from molybdenum d orbitals. Additional peaks are evident at $17.0 \pm 0.2$ eV and at $12.5 \pm 0.2$ eV and are assigned to emission from the $\sigma_{SS}$ and $\sigma^*_{SS}$ molecular orbitals of ethylene respectively, yielding a peak spacing $\Delta(\sigma_{SS}-\sigma^*_{SS}) = 4.5 \pm 0.2$ eV. Note that the photon energy was selected to enhance the intensity of these levels. Marked as vertical lines below these spectra are the peak positions in the gas-phase photoelectron spectrum of ethylene. As the sample temperature increases, the intensities of the peaks at 17.0 and 12.5 eV decrease so that after the sample has been annealed to $\sim 250$ K, these features are completely absent leaving only oxygen photoemission features. The corresponding temperature-programmed desorption spectra obtained by exposing a $MoO_2$ sample to ethylene (5 L exposure) at 80 K and collecting the spectrum at a heating rate of 10 K $s^{-1}$ are displayed in Fig. 2. These display a single 27 amu peak centered at 190 K and, in contrast to the chemistry found on oxygen-covered Mo(100) (see below), no other desorbing species were detected. The 2 amu signal is ascribed to mass spectrometer ionizer fragmentation of ethylene and the relative intensities of these peaks agree well with the corresponding mass spectrometer ionizer fragmentation pattern of ethylene. This indicates that ethylene merely adsorbs and desorbs molecularly on $MoO_2$. A simple Redhead analysis of this desorption state using a typical pre-exponential factor of $1 \times 10^{13}$ $s^{-1}$ yields a desorption activation energy of $\sim 11.1$ kcal $mol^{-1}$.

Shown in Fig. 3 are the photoelectron spectra of ethylene adsorbed on oxygen-covered Mo(100) at various temperatures where the oxygen coverage is 0.2 ML and shown for comparison is the spectrum of an oxygen-covered surface prior to ethylene exposure. Annealing temperatures are displayed adjacent to their corresponding spectra. Features are evident at $17.5 \pm 0.2$ eV and at $13.2 \pm 0.2$ eV and are assigned to emission from

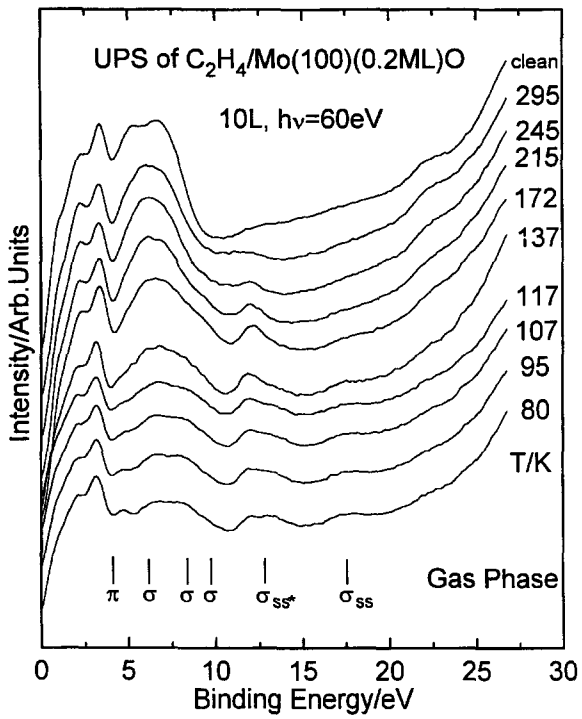


Fig. 3. Ultraviolet photoelectron spectra displaying the carbon and oxygen 2s region obtained following ethylene adsorption (10 L) on a Mo(100) surface covered with 0.2 ML of oxygen as a function of sample annealing temperature. The annealing temperature is displayed adjacent to the corresponding spectrum. These spectra were excited using 60-eV photons.

the $\sigma_{ss}$ and $\sigma^*_{ss}$ molecular orbitals of ethylene respectively, yielding a peak spacing $\Delta(\sigma_{ss}-\sigma^*_{ss}) = 4.2 \pm 0.2$ eV. Also marked as vertical lines below these spectra are the peak positions for gas-phase ethylene and features in the spectrum at 80 K can be straightforwardly associated with gas-phase peaks. It is evident that the $\sigma_{ss}$–$\sigma^*_{ss}$ spacing is somewhat smaller following adsorption on O/Mo(100) than the corresponding gas-phase values indicating a lengthening of the carbon–carbon bond. A similar behavior is found on clean Mo(100) where adsorbed ethylene is substantially rehybridized so that the carbon is $\sim sp^3$. Additional structure is evident between $\sim 5$ and 10 eV BE which is assigned to ethylene 2p-derived energy levels although these are obscured by the O 2p feature. Evident at $\sim 4.5$ eV BE is a small peak assigned to emission from the ethylenic $\pi$ orbital which is stabilized relative to the corresponding gas-phase value due to bonding to the surface. As the surface is heated, the intensities of the features due to the adsorption of ethylene decrease and a feature appears at $\sim 11.8$ eV. This is assigned to emission from a surface $C_1$ species and its binding energy agrees well with that found for carbene species grafted onto oxygen-covered Mo(100) by decomposing methylene iodide [23]. Note that there is evidence for this peak even following ethylene adsorption at 80 K. A similar $C_1$ formation reaction is found for ethylene on metallic Mo(100) although no dissociation is found until the sample is heated to above 80 K.

The corresponding photoelectron spectra for ethylene adsorbed on a Mo(100) surface covered with 0.83 ML of oxygen are displayed as a function of annealing temperature in Fig. 4. Again, oxygen-induced photoemission features are evident at 22.5 eV and between 5 and 10 eV BE and C

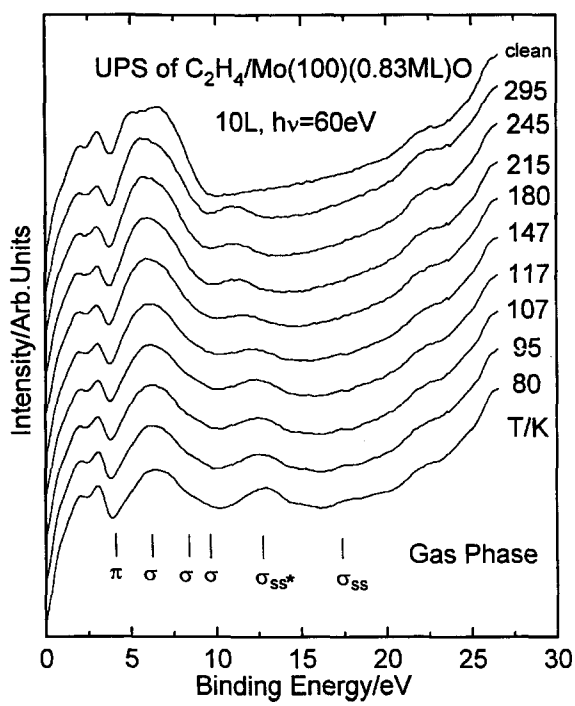


Fig. 4. Ultraviolet photoelectron spectra displaying the carbon and oxygen 2s region obtained following ethylene adsorption (10 L) on a Mo(100) surface covered with 0.83 ML of oxygen as a function of sample annealing temperature. The annealing temperature is displayed adjacent to the corresponding spectrum. These spectra were excited using 60-eV photons.

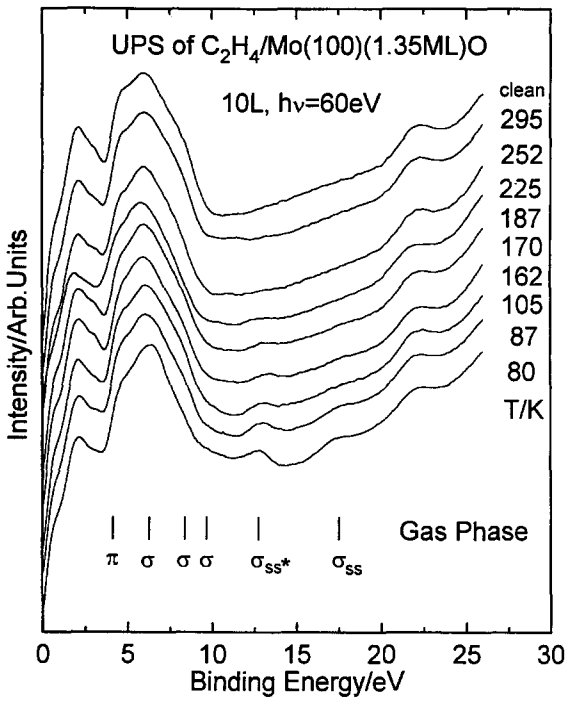


Fig. 5. Ultraviolet photoelectron spectra display the carbon and oxygen 2s region obtained following ethylene adsorption (10 L) on a Mo(100) surface covered with 1.35 ML of oxygen as a function of sample annealing temperature. The annealing temperature is displayed adjacent to the corresponding spectrum. These spectra were excited using 60-eV photons.

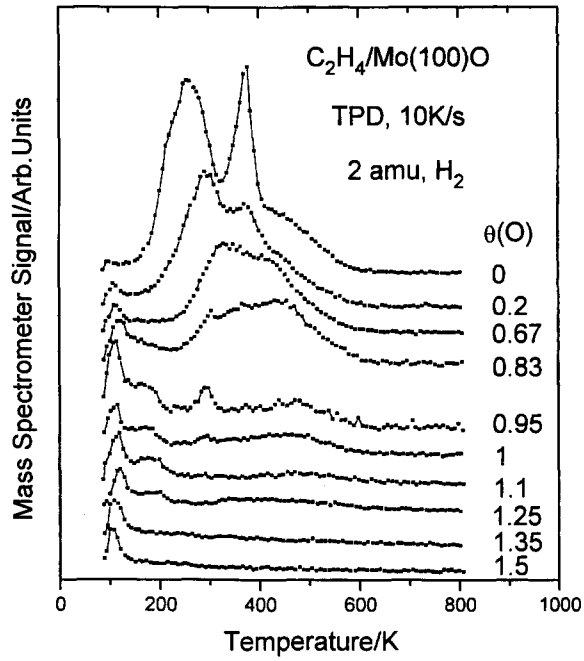


Fig. 6. Hydrogen (2 amu) temperature-programmed desorption spectra collected after saturating various oxygen-covered surfaces of Mo(100) with ethylene. The oxygen coverages are displayed adjacent to the corresponding spectrum.

2s-derived levels are clearly visible at ~17.6 eV and 13.1 eV. As the sample is heated, these features decrease in intensity to be replaced by a single feature with a binding energy of ~11 eV. This value compares well with the binding energy of carbene species on oxygen-covered Mo(100) formed by methylene iodide decomposition [23]. The intensity of the 13.1 eV feature is substantially larger than that of the 17.6 eV peak again indicating the dissociative adsorption of ethylene even at relatively low temperatures on this surface.

Finally, shown in Fig. 5 is the photoelectron spectrum for Mo(100) covered with 1.35 ML of oxygen. Again this displays intense features due to adsorbed oxygen at 22.5 eV and between 5 and 10 eV binding energy and peaks are evident at ~17.5 and ~12.7 eV due to emission from C 2s-derived orbitals. The ethylene-derived features again decrease in intensity as a function of annealing temperature. There is clearly significantly less ethylene adsorbed on the surface at such high oxygen coverages and the 12.7 and 17.5 eV peaks are closer in intensity suggesting that this surface may be less reactive toward C=C bond scission than surfaces with lower oxygen coverages.

The hydrogen (2 amu) desorption spectra for various oxygen-covered surfaces are displayed in Fig. 6. Clean Mo(100) exhibits two features at ~250 K and 380 K. The 250 and 380 K features shift to higher temperatures as the oxygen coverage increases. The small features at ~180 and 300 K at higher oxygen coverages are ascribed to the mass spectrometer ionizer fragmentation of ethylene (see Fig. 7)

The corresponding ethylene (27 amu) desorption spectra are displayed in Fig. 7. The nature of this species was confirmed by comparing the area under the desorption trace at various masses with the mass spectrometer ionization pattern of ethylene itself, where good agreement was found with both that measured by leaking ethylene into the vacuum

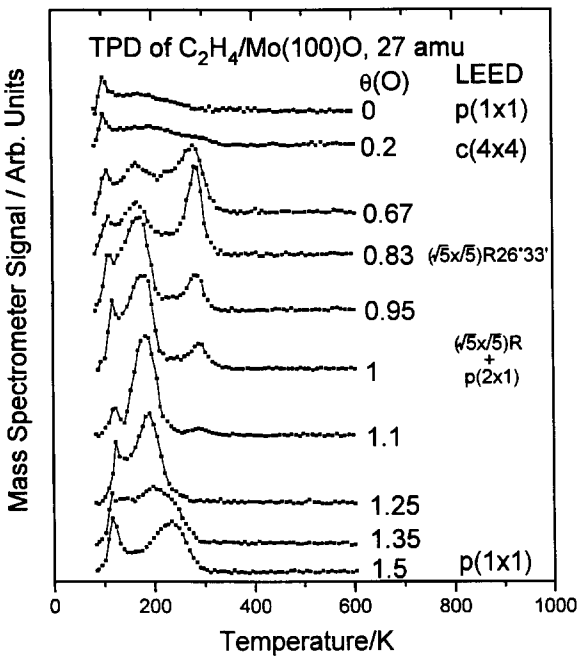


Fig. 7. Ethylene (27 amu) temperature-programmed desorption spectra collected after saturating various oxygen-covered surfaces of Mo(100) with ethylene. The oxygen coverages and their LEED patterns are displayed adjacent to the corresponding spectrum.

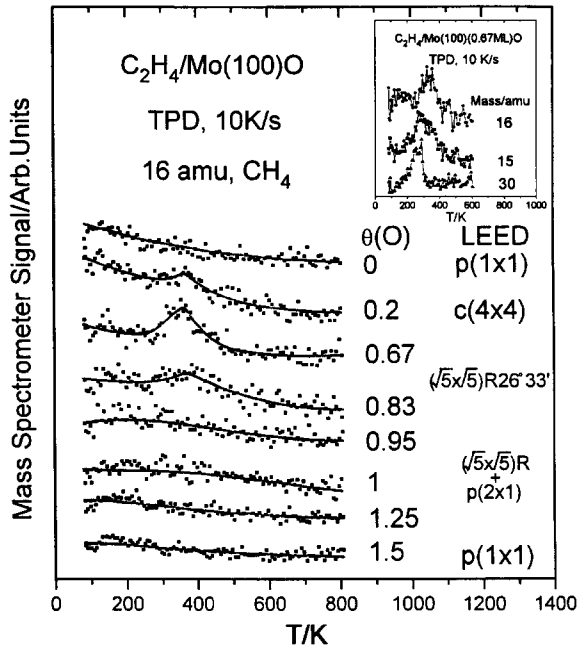


Fig. 8. Methane (16 amu) temperature-programmed desorption spectra collected after saturating various oxygen-covered surfaces of Mo(100) with ethylene. The oxygen coverages and their LEED patterns are displayed adjacent to the corresponding spectrum. The inset shows the corresponding 15 and 30 amu spectra demonstrating that the 350 K, 16 amu desorption peak is due to methane.

chamber and with literature values. The shape of this curve varies significantly as a function of oxygen exposure and displays a broad peak at ~200 K for the clean surface which shifts slightly with the addition of 0.2 ML of oxygen. This peak becomes sharper and more intense appearing at 280 K as the oxygen coverage increases to 0.67 ML with an additional peak appearing at 170 K. At 0.83 ML, the high-temperature peak shifts further to ~290 K and becomes substantially narrower and the 170 K peak increases slightly in intensity. At 0.95 ML the high-temperature peak increases in temperature and becomes even narrower and then decreases substantially in intensity as the oxygen coverage increases to 1.0 ML. The low-temperature peak shifts to higher temperatures with increasing oxygen coverage so that for a coverage of 1.5 ML, the spectrum exhibits a peak at ~220 K. This peak shift for high oxygen coverages on Mo(100) has been observed previously and ascribed to a change in Lewis acidity of the surface because of the effect of adsorbed oxygen [29,30]. Note in this case, that the integrated area under the ethylene desorption trace does not change substantially with increasing oxygen coverage except for $\theta(O)=0$ and 0.2 ML surfaces. Finally, displayed adjacent to each of the spectra are the oxygen LEED patterns displayed for each of the oxygen coverages. These correspond well with the results from other authors [24–27].

Methane was also found to desorb from some of the oxygen-covered surfaces. Note that ultraviolet photoelectron spectroscopic data for ethylene adsorbed on Mo(100) show that ethylene can dehydrogenate to form acetylene and also undergoes carbon–carbon bond scission to form surface $C_1$ species [20]. It has also been shown that methylene species adsorbed on clean and oxygen-covered Mo(100) [23] and clean Mo(110) [31] can react with surface hydrogen to form methane. Methane desorption is found following

ethylene adsorption on O/Mo(100) but only in a narrow oxygen coverage range. These results are illustrated in Fig. 8 which displays the methane (16 amu) desorption spectra obtained after saturating various oxygen-covered Mo(100) surfaces with ethylene. The desorption of methane was confirmed by comparing the desorption intensity with the mass spectrometer ionizer fragmentation pattern for methane and the corresponding 15 and 16 amu peaks are shown as an inset. 15 amu is also a fragment of ethane which is formed as a self-hydrogenation product (see below) so that the corresponding ethane (30 amu) feature is also displayed in the inset. Part of the 15 amu intensity is also due to fragmentation of ethane but when this contribution is subtracted from the 15 amu peak, good agreement is obtained with the expected methane fragmentation intensity. There is no detectable methane desorption for clean Mo(100), in spite of the detection of surface $C_1$ species using ultraviolet photoelectron spectroscopy. Note, however, that carbenes formed by methylene iodide decomposition do hydrogenate to methane on clean Mo(100). However, increasing the oxygen coverage to 0.2 ML results in a small amount of methane desorption at ~370 K. The amount of methane formed increases further as the oxygen coverage is increased to 0.67 ML and then decreases slightly as the oxygen coverage increases to 0.83 ML. No further methane is found for increasing oxygen coverages.

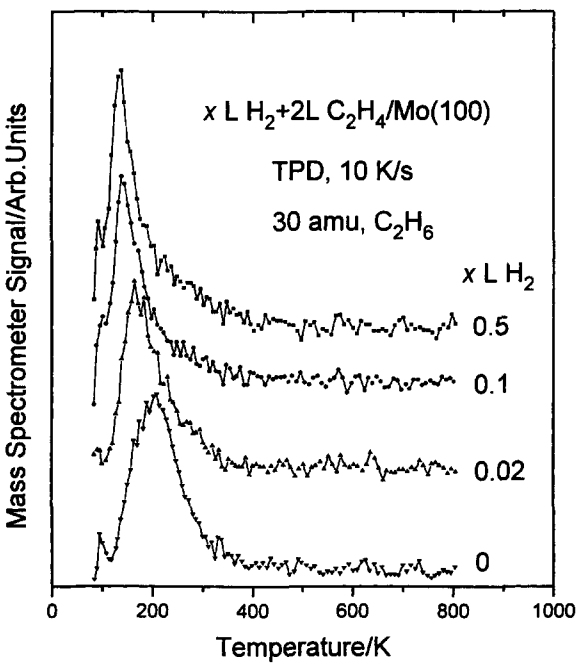


Fig. 9. Ethane (30 amu) temperature-programmed desorption spectra obtained following various exposures of a Mo(100) surface to hydrogen and then a to 2 L ethylene. Hydrogen exposures are displayed adjacent to the corresponding spectrum.

Self-hydrogenation of ethylene to form ethane is also detected on molybdenum and oxygen-covered molybdenum. It has been shown previously that metallic molybdenum can catalyze ethylene hydrogenation [32]. The temperature-programmed desorption spectrum of ethane formed by ethylene adsorption on Mo(100) is shown in Fig. 9 and reveals a single peak centered at 210 K. The effect of pre-dosing the clean surface with hydrogen is also shown in these spectra, where there is apparently no substantial increase in the ethane desorption yield but there is a drastic decrease in the desorption peak temperature so that pre-dosing the surface with 0.5 L of hydrogen yields a peak centered at 120 K. Note that the shape of the desorption state also changes substantially as the hydrogen pre-coverage increases.

Ethane desorption spectra are displayed in Fig. 10 as a function of oxygen coverage. Clearly, the amount of ethane formed by self-hydrogenation decreases substantially with increasing oxygen coverage so that for 1.0 ML of oxygen, essentially no ethane is formed. In addition, the desorption peak temperature increases with increasing oxygen coverage so that for 0.95 ML of oxygen, the peak is at ~300 K.

Finally, no other species, for example, oxygen-containing molecules or water, were found to desorb from any of the oxygen-covered surfaces. Catalytic results also suggest that, at least at high reaction temperatures, metathesis can proceed via the recombination of surface $C_1$ species. In order to examine whether a similar chemistry operates on oxygen-covered Mo(100) in ultra-high vacuum, it was exposed to isotopically labelled $^{13}C^{12}CH_4$ and TPD spectra collected at 30 amu ($^{13}C^{13}CH_4$), 29 amu ($^{13}C^{12}CH_4$) and 28 amu ($^{12}C^{12}CH_4$). No isotope scrambling was noted in any case.

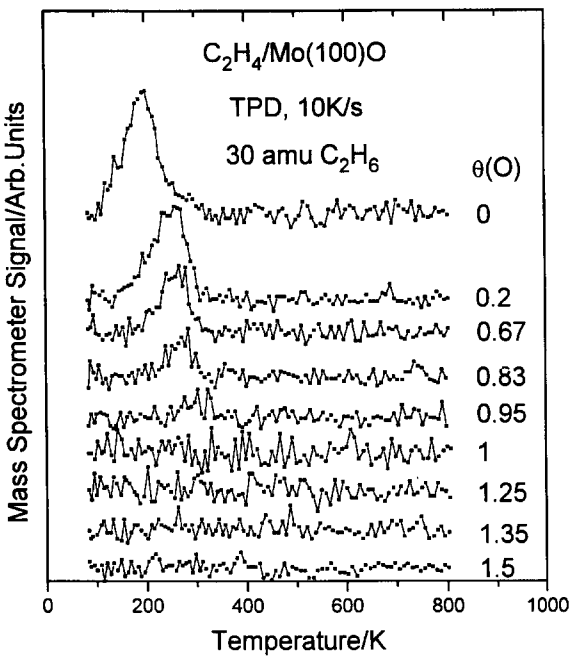


Fig. 10. Ethane (30 amu) temperature-programmed desorption spectra collected after saturating various oxygen-covered surfaces of Mo(100) with ethylene. The oxygen coverages are displayed adjacent to the corresponding spectrum.

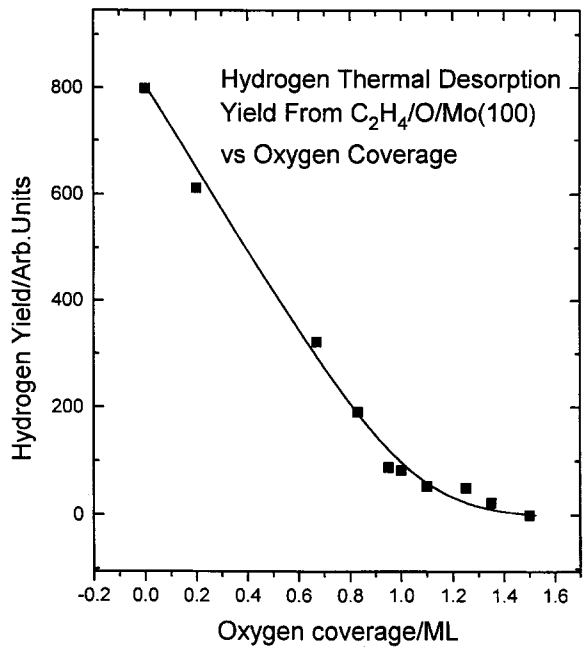


Fig. 11. Plot of the total hydrogen thermal desorption yield from ethylene adsorbed onto oxygen-covered Mo(100) as a function of oxygen coverage.

## 4. Discussion

Hydrogen (Fig. 6) is the major desorption product found following adsorption of ethylene on Mo(100) resulting from a total thermal decomposition of adsorbed ethylene to form carbon and hydrogen. Note that the data of Fig. 7 show that the amount of ethylene desorbing from the surface remains reasonably constant except for $\theta_O = 0$ and 0.2 ML. Plotted in Fig. 11 is the total hydrogen yield from an ethylene-saturated surface (obtained by integrating the 2 amu TPD data of Fig. 6) as a function of oxygen coverage where any contribution to this curve due to the fragmentation of other species in the mass spectrometer ionizer (primarily ethylene) has been subtracted. The graph decreases linearly with increasing oxygen coverage up to an oxygen coverage of unity, where the hydrogen desorption yield decreases essentially to zero. This implies that the sites at which ethylene decomposes are being directly blocked by oxygen. Note that ethylene adsorbed on $MoO_2$ yields essentially no hydrogen in accord with this trend (Fig. 2). It has been shown, at least for lower oxygen coverages, that oxygen adsorbs in the four-fold hollow site on Mo(100) [33] so that the data of Fig. 11 imply that these sites are being blocked to suppress ethylene dehydrogenation. This observation follows the general pattern for chemistry on Mo(100) where the four-fold hollow site is substantially more reactive than other sites so that, for example, CO adsorbed in the four-fold hollow sites dissociates into carbon and oxygen whereas CO adsorbs and desorbs molecularly on the atop site [34]. In addition, comparison of the hydrogen desorption yield for ethylene on clean Mo(100) with the yield of hydrogen from the same surface yields an effective ethylene coverage for desorption from this site of 1.0. These results taken together suggest that all of the ethylene adsorbed in four-fold hollow sites completely thermally decomposes to yield hydrogen and deposit carbon. Note that acetylenic species are also detected on this surface [20] so that dehydrogenation may take place via this intermediate although no acetylene is found to desorb.

The photoelectron spectroscopic data of Figs. 3–5 for oxygen-covered Mo(100) surfaces all indicate that the two peaks measured following ethylene adsorption at 80 K and assigned to emission from the $\sigma_{SS}$ and $\sigma^*_{SS}$ orbitals coalesce into a single level on heating indicating the formation of adsorbed $C_1$ species on the surface. This effect has been observed previously for ethylene adsorbed on metallic Mo(100). The $\sigma_{SS}$–$\sigma^*_{SS}$ spacing for gas-phase ethylene is 4.5 eV [35,36]. Rehybridization to $sp^3$ would yield a corresponding value of 4.7 eV [20] and this suggests that adsorbed ethylene is rehybridized following adsorption on an oxygen-modified Mo(100) surface. Formation of surface $C_1$ species is confirmed by the desorption of methane from the surface due to hydrogenation of adsorbed $CH_x$ groups. In addition, the data of Figs. 3 and 4 indicate that $C_1$ species may form even following adsorption at 80 K on surfaces with oxygen coverages of 0.2 and 0.83 ML which suggests that adsorbed oxygen increases the reactivity of the molybdenum surface toward C=C bonds scission. $CH_2$ hydrogenation has been detected previously on Mo(100) and oxygen-covered Mo(100) where carbenes were formed by thermally decomposing methylene iodide on these surfaces [23]. Interestingly, in those cases, methane is formed at substantially lower temperatures ($\sim$200 K) than the temperature of $\sim$370 K found in this case. The origin of this effect is not entirely clear. One possibility is that carbenes grafted onto the surface by the decomposition of methylene iodide have iodine atoms adsorbed onto the surface close to them which might affect the kinetics of hydrogenation to methane. Note however that the presence of an oxygen overlayer does not substantially effect the methane formation kinetics so it is difficult to understand how adsorbed iodine could have such a substantial effect. Another possibility is that the methane formation rate from adsorbed ethylene is not limited by the rate of carbene hydrogenation but by the rate at which carbenes are formed by carbon–carbon bond dissociation. However, the ultraviolet photoelectron spectra of ethylene on the various surfaces suggests that the onset of $C_1$ formation is at about 80 K, substantially lower than the methane desorption features.

It is also found that the carbene stability is substantially affected by the presence of oxygen; the larger the oxygen coverage, the more stable the carbene. Thus, the activation energy for carbene decomposition increases substantially with increasing oxygen coverage [23]. Note that there is a 2 amu feature at approximately 350 K (Fig. 6) which might be due to carbene decomposition. Thus, the variation in methane yield as a function of oxygen coverage (Fig. 8) can be rationalized rather straightforwardly using these ideas. First, the dissociative adsorption probability on the surface increases with increasing oxygen coverage and second, the resulting carbene is stabilized by increasing the oxygen coverage.

As the oxygen coverage increases further, the methane yield decreases once again. This result is likely due either to the lack of available hydrogen obtained from ethylene dehydrogenation on the surface since the number of available four-fold sites decreases (Fig. 11) or to a lack of reactivity of the ethylene toward carbene formation as the oxygen coverage increases. Further evidence for these effects come from the data of Fig. 10 which show the variation in ethane yield due to the self-hydrogenation of adsorbed ethylene where the hydrogen derives from ethylene that decomposes on the surface. In this case there is a decrease in the amount of ethane that is formed with increasing oxygen coverage. Here, the reactant ethylene is not formed from any other precursor (as was necessary in the case of methane formation) so is present in substantial amounts on clean Mo(100). The data of Fig. 9 demonstrate that, in this case, the hydrogen required to form ethane derives from the molybdenum surface since the ethane desorption spectrum is significantly altered by pre-dosing hydrogen. In this case, the peak temperature decreases with increasing hydrogen exposure.

A change in peak temperature of ethylene desorption (from 170 to 220 K; Fig. 7) is found in changing the oxygen coverage from $\sim$0.9 to 1.5 ML. This has been ascribed to the effect of a change of surface molybdenum oxidation state so that a $\theta_O = 1.0$ ML surface has an effective oxidation state of +2 and a 1.5 ML surface has an effective oxidation state of +4 [37]. Increased ethylene stabilization with increasing oxygen coverage

implies that, within the context of the Dewar-Chatt-Duncanson model, adsorption is primarily *via* donation of adsorbate $\pi$ electrons to the metal surface since the addition of an electron withdrawing co-adsorbate increases the ethylene stability. A similar change is noted in increasing the oxygen coverage from zero (the clean surface) where ethylene desorbs at 200 K, to about a monolayer where ethylene desorbs at $\sim$300 K (Fig. 7). In addition, the ethane formation temperature increase from 190 to $\sim$300 K as the oxygen coverage changes from 0 to 1.0 ML is in accord with this notion. This effect has been observed previously for hydrocarbons on Mo(100) [38] and they similarly rationalized their observations in terms of an alkene bonding primarily *via* donation of $\pi$ electrons to the surface. Note that the concomitant removal of electrons from the $\pi$ bonding orbitals will also have the effect of weakening the carbon–carbon bond enhancing the ethylene dissociation probability.

It has been shown above that essentially all of the ethylene adsorbed in the four-fold sites thermally decomposes to yield carbon and hydrogen. This suggests that ethylene desorbs from either atop or bridge sites and that these are effected by the presence of oxygen adsorbed in the four-fold sites. The sites occupied by ethylene at lower oxygen coverages from which ethylene desorbs at about 300 K depending on oxygen coverage are clearly blocked for oxygen coverages above a monolayer. At these higher coverages, another site is stabilized so that at an oxygen coverage of 0.95, ethylene desorbs from it at $\sim$170 K. As the oxygen coverage increases further, this site is further stabilized. Further work must be done to identify the exact nature of each of these sites. It should also be noted that the high-temperature ($\sim$300 K) peak (Fig. 7) which appears for oxygen coverages between 0.67 and 1.0 ML disappears abruptly for oxygen coverages above 1.1 ML. The presence of this species coincides with a $\sqrt{5}\times\sqrt{5}$ surface reconstruction so this desorption state may be associated with this surface.

## 5. Conclusions

Ethylene adsorbed on Mo(100) and oxygen-covered Mo(100) can thermally decompose to yield hydrogen, hydrogenate to form ethane, dissociate and hydrogenate to give methane or desorb. All of these reactions are affected by the presence of oxygen on the surface. Total thermal decomposition, as indicated by the yield of hydrogen as a function of oxygen coverage, appears to take place at the four-fold hollow sites on Mo(100) which are blocked by oxygen thus preventing thermal decomposition. The methane yield varies strongly with oxygen coverage so that no methane is formed on the clean surface. The yield increases with increasing oxygen coverage to reach a maximum at $\theta_O = 0.67$ ML and decreases at higher coverages. This variation in methane yield is associated with an increase in the stability of the carbene and an enhancement in the activity of the surface by the addition of oxygen. The yield decreases at higher coverage because of a lack of surface hydrogen.

The activation energy for ethylene desorption is found to increase with increasing oxygen coverage. This effect has been noted previously and rationalized by suggesting that ethylene adsorbs on molybdenum by donation of $\pi$ electrons of ethylene into the vacant substrate orbitals of molybdenum.

## Acknowledgements

We gratefully acknowledge support of this work by the U.S. Department of Energy, Division of Chemical Sciences, Office of Basic Energy Sciences, under Grant No. DE-FG02-92ER14289. This work is based upon research conducted at the Synchrotron Radiation Center, Univ. of Wisconsin-Madison, which is supported by the NSF under Award No. DMR-95-31009.

## References

[1] A.J. Gellman, M.H. Farias, G.A. Somorjai, J. Catal. 88 (1984) 564.
[2] A.J. Gellman, M.H. Farias, G.A. Somorjai, Surf. Sci. 136 (1984) 217.
[3] J.C. Mol, J.A. Moulijn, Adv. Catal. 24 (1975) 131.
[4] J. Höcker, W. Reimann, L. Reif, K. Riebel, J. Mol. Catal. 191 (1980).
[5] B. Bartlett, C. Soto, R. Wu, W.T. Tysoe, Catal. Lett. 21 (1993) 1.
[6] W.T. Tysoe, Langmuir 12 (1996) 78.

[7] J.L. Hèrison, Y. Chauvin, Makromol. Chem. 141 (1970) 161.
[8] R.J. Haines, G.J. Leigh, Chem. Soc. Rev. 4 (1975) 155.
[9] E.O. Fischer, K.H. Dotz, Chem. Ber. 105 (1972) 3966.
[10] R.R. Schrock, J. Am. Chem. Soc. 98 (1976) 5399.
[11] R.H. Grubbs, D.D. Carr, C. Hoppin, P.C. Burk, J. Am. Chem. Soc. 98 (1976) 3478.
[12] J.J. Katz, J. Rothschild, J. Am. Chem. Soc. 98 (1976) 2519.
[13] C.P. Casey, H. Tuinstra, M.C. Saeman, J. Am. Chem. Soc. 98 (1976) 608.
[14] F.N. Tebbe, G.W. Parshall, D.W. Ovenall, J. Am. Chem. Soc. 101 (1979) 5074.
[15] T.R. Howard, J.B. Lee, R.H. Grubbs, J. Am. Chem. Soc. 102 (1980) 6878.
[16] R.L. Banks, G.C. Bailey, Ind. Eng. Chem. Prod. Res. Dev. 94 (1965) 60.
[17] B. Bartlett, H. Molero, W.T. Tysoe, submitted to Catal. Lett.
[18] B. Bartlett, V.L. Schneerson, W.T. Tysoe, Catal. Lett. 3 (1995) 1.
[19] B. Bartlett, W.T. Tysoe, Catal. Lett., to be published.
[20] L.P. Wang, W.T. Tysoe, Surf. Sci. 236 (1990) 325.
[21] L.P. Wang, R. Hinkelman, W.T. Tysoe, J. Electron Spec. Rel. Phenom. 56 (1991) 341.
[22] L.P. Wang, W.T. Tysoe, Surf. Sci. 230 (1990) 74.
[23] G. Wu, B. Bartlett, W.T. Tysoe, Surf. Sci. 373 (1997) 129.
[24] H.M. Kennett, A.E. Lee, Surf. Sci. 48 (1975) 606.
[25] E.I. Ko, K.J. Madix, Surf. Sci. 109 (1981) 221.
[26] E. Bauer, H. Hoppa, Surf. Sci. 88 (1979) 31.
[27] C. Zhang, M.A. Van Hove, G.A. Somorjai, Surf. Sci. 149 (1985) 326.
[28] H.M. Kennett, A.E. Lee, Surf. Sci. 48 (1975) 624.
[29] J.E. Deffeyes, A.H. Smith, P.C. Stair, Appl. Surf. Sci. 26 (1986) 517.
[30] J.E. Deffeyes, A.H. Smith, P.C. Stair, Surf. Sci. 163 (1985) 79.
[31] M.K. Weldon, C.M. Friend, Surf. Sci. 321 (1994) L202.
[32] L. Wang, W.T. Tysoe, J. Catal. 128 (1991) 320.
[33] S.H. Overbury, P.C. Stair, J. Vac. Sci. Technol. A1 (1983) 1055.
[34] J.P. Fulmer, W.T. Tysoe, F. Zaera, J. Chem. Phys. 87 (1987) 4147.
[35] D.G. Streets, A.W. Potts, J. Chem. Soc. Faraday II 70 (1974) 1505.
[36] C.R. Brundle, M.B. Robin, H. Basch, M. Pinsky, A. Bond, J. Am. Chem. Soc. 92 (1970) 3863.
[37] J.L. Grant, T.B. Fryberger, P.C. Stair, Surf. Sci. 159 (1985) 333.
[38] J.L. Grant, T.B. Fryberger, P.C. Stair, Surf. Sci. 239 (1990) 127.